http://app.pan.pl/SOM/app58-Foth_Rauhut_SOM.pdf

SUPPLEMENTARY ONLINE MATERIAL FOR

Macroevolutionary and morphofunctional patterns in theropod skulls: a morphometric approach

Christian Foth and Oliver W.M. Rauhut

Published in *Acta Palaeontologica Polonica* 2013 58 (1): 1-16.
http://dx.doi.org/10.4202/app.2011.0145

Supplementary information

1. Taxon sampling

Table S1. List of taxa used in the present analyses with data of occurrences (in million of years, Ma) and sources of images.

Taxon	Systematic affinities	Age (Ma)	Sources
Euparkeria	Basal archosauriform	Anisian (241,5)	Rauhut 2003
Lesothosaurus	Ornithischia	Hettangian/Sinemurian (202)	Norman et al. 2004
Massospondylus	Sauropodomorpha	Sinemurian (198,5)	Gow et al. 1990
Plateosaurus	Sauropodomorpha	Norian (215,5)	Galton 1985
Herrerasaurus	Herrerasauridae	Carnian (224)	Langer 2004
Eoraptor	Basal theropod	Carnian (224)	Langer 2004
Daemonosaurus	Basal theropod	Rhaetian (208)	Sues et al. 2011
Syntarsus kayentakatae	Coelophysidae	Sinemurian/Pliensbachian (195)	Tykosky 1998
Coelophysis	Coelophysidae	Carnian/Norian (221)	Colbert 1989
Zupaysaurus	Basal neotheropod	Norian (215,5)	Ezcurra 2007
Limusaurus	Ceratosauria	Oxfordian (156,5)	Xu et al. 2009
Ceratosaurus	Ceratosauria	Kimmeridgian/Tithonian (151)	Sampson & Witmer 2007
Carnotaurus	Abelisauridae	Campanian/Maastrichtian (71,3)	Rauhut 2003
Majungasaurus	Abelisauridae	Campanian (77,4)	Sampson & Witmer 2007
Monolophosaurus	Megalosauroidea	Callovian (161,5)	Brusatte et al. 2010
Spinosaurid	Megalosauroidea	Albian (105,5)*	Rauhut 2003
Sinraptor	Allosauroidea	Oxfordian (156,5)	Currie & Zhao 1993
Acrocanthosaurus	Allosauroidea	Aptian/Albian (112)	Eddy & Clarke 2011
Allosaurus	Allosauroidea	Kimmeridgian/Tithonian (151)	Rauhut 2003
Guanlong	Tyrannosauroidea	Oxfordian (156,5)	Xu et al. 2006
Dilong	Tyrannosauroidea	Barremian (124)	Xu et al. 2004
Bistahieversor	Tyrannosauroidea	Campanian (77,4)	Carr & Williamson 2010
Alioramus	Tyrannosauridae	Maastrichtian (68,15)	Brusatte et al. 2009
Daspletosaurus	Tyrannosauridae	Campanian (77,4)	Holtz 2004
Gorgosaurus	Tyrannosauridae	Campanian (77,4)	Rauhut 2003
Tarbosaurus	Tyrannosauridae	Campanian/Maastrichtian (71,3)	Hurum & Sabbath 2003
Tyrannosaurus	Tyrannosauridae	Campanian/Maastrichtian (71,3)	Holtz 2004
Compsognathus	Compsognathidae	Kimmeridgian (152,5)	Peyer 2006
Garudimimus	Ornithomimosauria	Cenomanian-Santonian (89)	Makovicky et al. 2004
Gallimimus	Ornithomimosauria	Maastrichtian (68,15)	Makovicky et al. 2004
Ornithomimus	Ornithomimosauria	Campanian/Maastrichtian (71,3)	Rauhut 2003
Erlikosaurus	Therizinosauridae	Cenomanian-Santonian (89)	Rauhut 2003
Conchoraptor	Oviraptoridae	Campanian (77,4)	Osmolska et al. 2004
Citipati	Oviraptoridae	Campanian (77,4)	Osmolska et al. 2004
Oviraptor	Oviraptoridae	Campanian (77,4)	Osmolska et al. 2004
Archaeopteryx	Avialae	Kimmeridgian (152,5)	Rauhut 2003

Confuciusornis	Avialae	Barremian (124)	Chiappe et al. 1999
Pengornis	Avialae	Barremian (124)	O'Connor & Chiappe 2011
Shenquiornis	Avialae	Barremian (124)	O'Connor & Chiappe 2011
Anchiornis	Troodontidae	Oxfordian (156,5)	Hu et al. 2009
Sinornithosaurus	Dromaeosauridae	Barremian (124)	Xu & Wu 2001
Bambiraptor	Dromaeosauridae	Campanian (77,4)	Burnham 2004
Velociraptor	Dromaeosauridae	Campanian (77,4)	Barsbold & Osmolska 1999
Shuvuuia	Alvarezsauridae	Campanian (77,4)	Chiappe et al. 2002

*The reconstruction of a generalized spinosaurid is based on several taxa (the orbital and postorbital region mainly based on *Irritator*, and the snout based on *Suchomimus*, with some elements reconstructed after *Baryonyx*; see Rauhut 2003), which range in age from the Barremian to the Cenomanian, so we used an intermediate stage between these extremes for the age estimate of this reconstruction.

2. Description of landmarks

Homologous landmarks plotted on all theropod skulls in lateral view. The landmarks present in both data sets are bold. Landmark 21 is only present in the smaller data set (latin). Marked (*) landmarks are identical with Brusatte et al. (2012).

1. **anteroventral corner of the premaxilla (this point is reconstructed in *Alioramus* and *Zupaysaurus* due to a missing premaxilla) (preorbital region) ***
2. **contact of premaxilla and nasal above the external naris (preorbital region) ***
3. **contact of premaxilla and maxilla along the tooth row (preorbital region) ***
4. **tip of the maxillary process of the premaxilla (preorbital region)**
5. **anterodorsal contact between lacrimal and nasal (preorbital region)**
6. **contact between maxilla and jugal along the margin of antorbital fenestra (in those taxa where the jugal do not reach the antorbital fenestra – the most anterior point of the jugal is chosen, as in most theropods the contact between maxilla and jugal along the antorbital fenestra is also the most anterior point of the jugal) (preorbital region)**
7. **contact of maxilla and jugal along the ventral margin of the skull (preorbital region) ***
8. **contact between lacrimal and jugal on the orbital margin (preorbital region)**
9. **contact between postorbital and jugal on the orbital margin (postorbital region) ***

10. contact between postorbital and jugal on the margin of the lateral temporal fenestra (postorbital region) *
11. contact between jugal and quadratojugal on the margin of the lateral temporal fenestra (postorbital region) *
12. anteroventral tip of the squamosal on the margin of the lateral temporal fenestra (postorbital region) *
13. ventral contact of postorbital and squamosal on the margin of the lateral temporal fenestra (postorbital region)
14. anterior tip of the postorbital on the orbital margin (postorbital region)
15. most-anterior point of the antorbital fenestra (preorbital region) *
16. dorsal contact between postorbital and squamosal (postorbital region)
17. posteroventral corner of the quadratojugal (postorbital region) *
18. posteroventral tip of the squamosal posterior process (postorbital region) *
19. most-ventral point of the orbit (postorbital region)
20. posterior tip of the lacrimal on the orbital margin (postorbital region)
21. *contact of the frontal with the parietal on the skull roof*

3. Biomechanical and ecological parameters

The respective skull lengths and depths were estimated with help of the program tpsDig2 (Rohlf 2005) using the measure mode. The skull length was measured from the anterior tip of the premaxilla to the posterior end of the quadratojugal. The skull depth was measured at the height of the orbit. The average maximum stress was estimated using the data from Rayfield (2011). To estimate the skull strength indicator (SSI) the original data from Henderson (2002) were used to calculate a regression between skull depth and SSI (see Fig. S1). The estimated average maximum stress based on a regression of the original data from Rayfield (2011) (see Fig. S2).

Table S2. List of taxa used for the functional and ecological analyses with relevant parameters. C carnivorous; H herbivorous; O omnivorous (herbivorous and omnivorous taxa are summarized in non-carnivorous taxa); G generalist; W weak-biting; S strong-biting.

Taxon	Skull lengths (cm)	Average maximum stress (N/m^2)	Skull depth (cm)	Skull strength indicator	Diet	Feeding ecology
Euparkeria	8.1	141.2	2.8	0.6	C	G
Lesothosaurus	6.4	107.4	2.4	0.5	O	G
Massospondylus	15.0	288.3	6.3	3.8	O	G
Plateosaurus	32.2	698.3	8.4	7.2	O	G
Herrerasaurus	29.7	636.1	8.8	7.9	C	G
Eoraptor	13.5	254.5	5.2	2.5	O	G
Daemonosaurus	13.4	251.2	6.9	4.7	C	G
Syntarsus	20.7	418.2	5.4	2.7	C	W
Coelophysis	21.0	425.0	7.4	5.5	C	W
Zupaysaurus	44.7	1023.6	13.3	19.4	C	W
Limusaurus	10.0	179.4	6.1	3.6	H	W
Ceratosaurus	68.8	1688.8	23.2	65.6	C	S
Carnotaurus	57.7	1377.3	38.1	193.4	C	S
Majungasaurus	55.7	1320.9	28.0	98.8	C	S
Monolophosaurus	66.6	1625.9	20.6	50.8	C	G
Spinosaurid	78.2	1958.1	22.0	58.4	C	W
Sinraptor	83.2	2104.5	30.0	114.9	C	S
Acrocanthosaurus	129.0	3506.4	50.9	363.8	C	S
Allosaurus	66.0	1608.3	23.3	66.4	C	S
Guanlong	33.2	724.6	9.0	8.3	C	G
Dilong	18.7	371.6	6.1	3.5	C	G
Bistahieversor	99.2	2584.6	30.6	119.9	C	S

Alioramus	62.0	1497.2	15.0	25.4	C	G
Daspletosaurus	103.4	2710.7	35.2	162.9	C	S
Gorgosaurus	102.3	2676.3	31.6	128.5	C	S
Tarbosaurus	127.1	3445.8	34.7	158.1	C	S
Tyrannosaurus	123.9	3347.0	51.1	366.0	C	S
Compsognathus	9.3	165.1	2.9	0.7	C	W
Garudimimus	24.8	514.7	9.9	10.2	H	W
Gallimimus	28.2	599.7	10.0	10.5	H	W
Ornithomimus	21.2	428.8	7.9	6.2	H	W
Erlikosaurus	21.3	432.8	6.6	4.2	H	G
Conchoraptor	8.7	152.4	4.1	1.5	O	S
Citipati	13.4	252.3	6.3	3.8	O	S
Oviraptor	17.1	335.4	7.9	6.2	O	S
Archaeopteryx	3.0	44.8	1.2	0.1	O	W
Confuciusornis	6.7	133.2	2.8	0.6	O	G
Anchiornis	5.4	87.3	3.0	0.8	O	W
Sinornithosaurus	13.7	258.5	4.5	1.9	C	G
Bambiraptor	11.2	205.3	3.7	1.2	C	G
Velociraptor	25.4	530.4	7.3	5.3	C	G
Pengornis	-	-	-	-	O	W
Shenquiornis	-	-	-	-	O	W
Shuvuuia	-	-	-	-	O	W

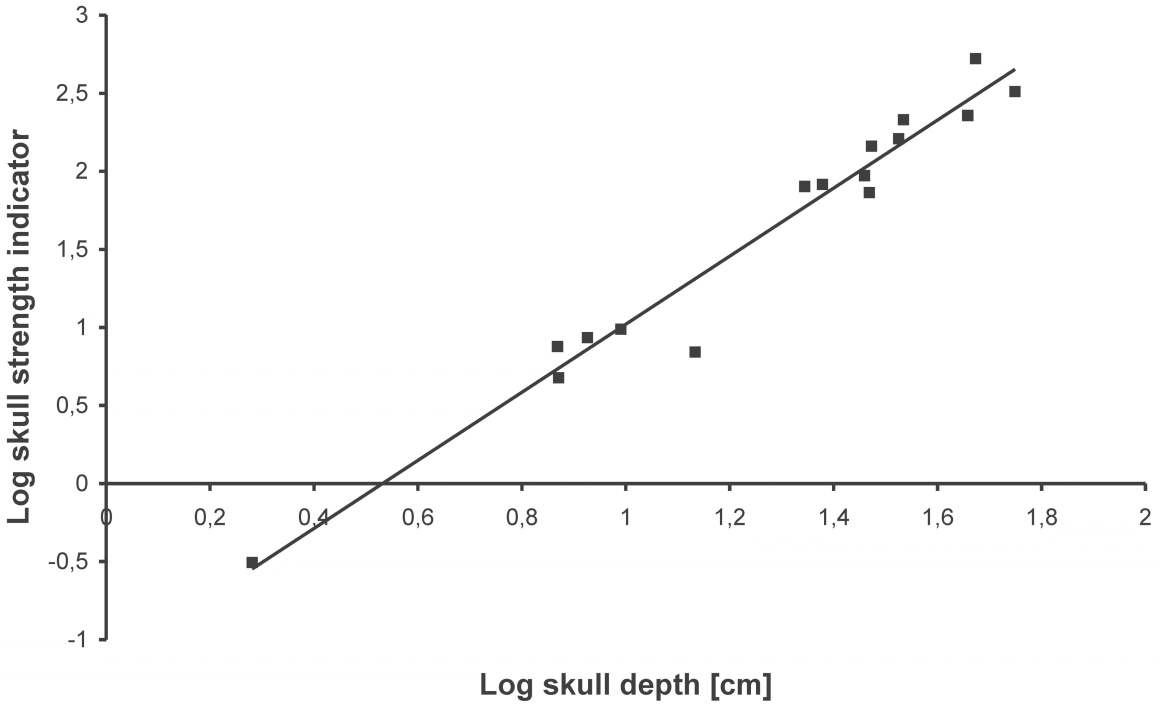

Fig. S1. Correlation between skull depth and skull strength indicator (LogSSI = 2.18 LogSD – 1.1602, $R^2 = 0.963$, *p*-value < 0.001) (based on the data set from Henderson 2002).

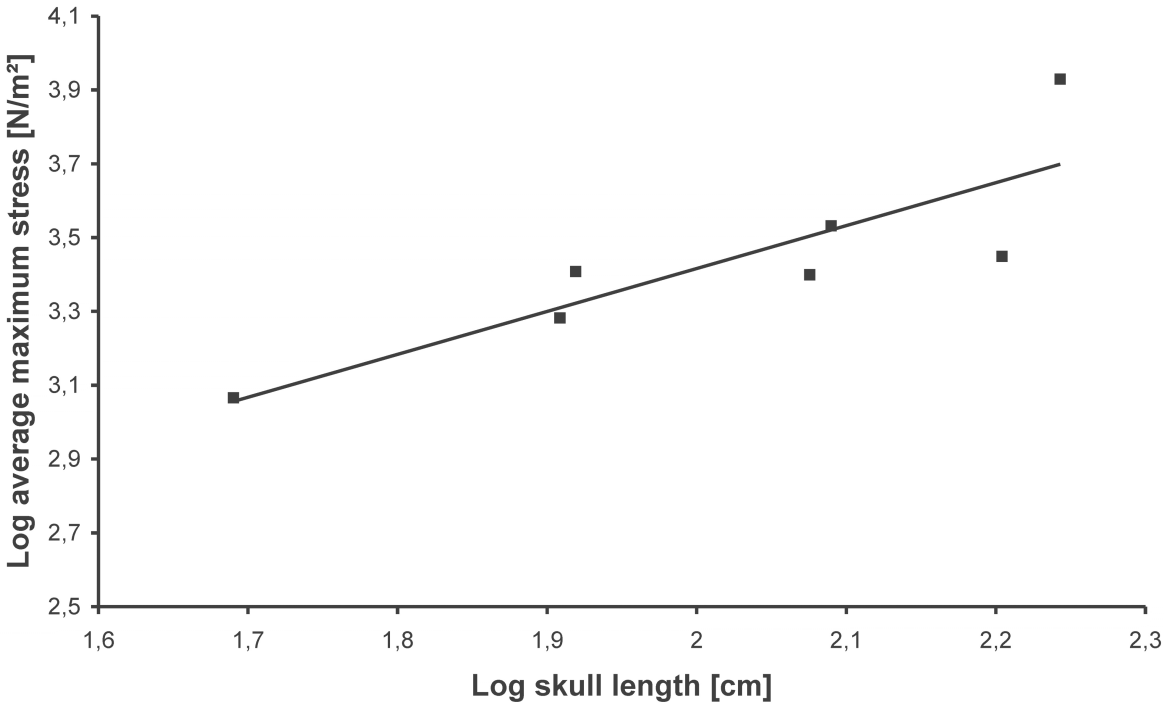

Fig. S2. Correlation between skull length and average maximum stress (LogAMS = 1.16 LogSL – 1.0913, $R^2 = 0.725$, *p*-value < 0.001) (based on the data set from Rayfield 2011, without a crestless *Monolophosaurus*).

Table S3. Correlation of specimen centroid size (log transformed) with Procrustes Coordinates and the first three PC axes.

	R^2	*p*-value
Procrustes Coordinates (large data set)	0.159	<0.001
Procrustes Coordinates (small data set – Paraves)	0.140	<0.001
PC 1 (large data set)	0.166	0.007
PC 1 (small data set – Paraves)	0.083	0.335
PC 2 (large data set)	0.452	<0.001
PC 2 (small data set – Paraves)	0.169	0.147
PC 3 (large data set)	0.163	0.009
PC 3 (small data set – Paraves)	0.139	0.188

4. Phylogeny and cluster topologies

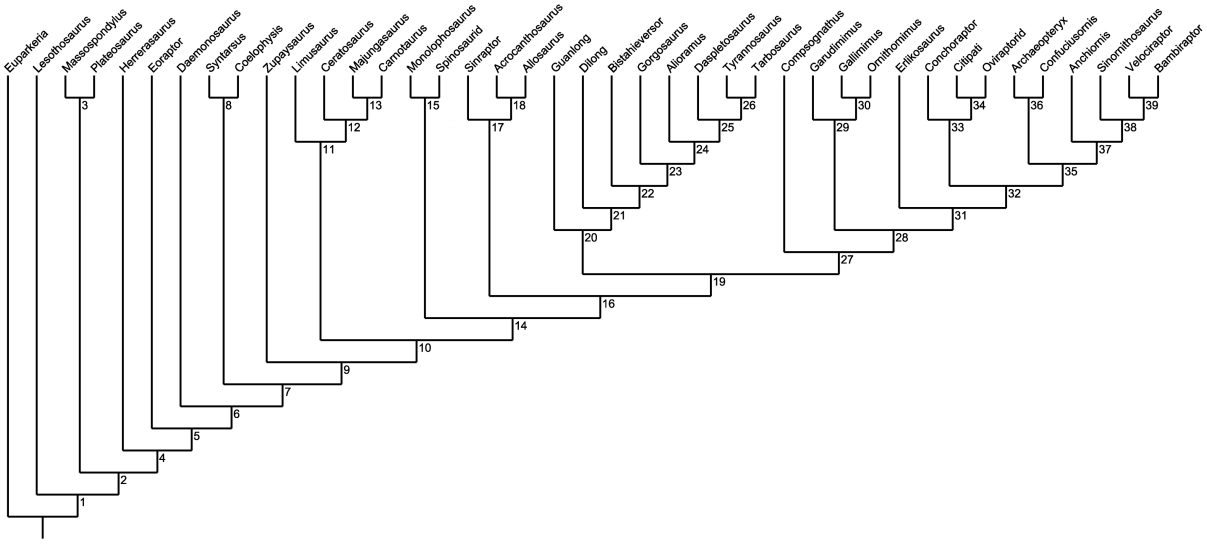

Fig. S3. Topology of the informal supertree used in all phylogenetic comparative analyses based on the large data set. 1 Dinosauria; 2 Saurischia; 3 Sauropodomorpha; 4 Theropoda; 7 Neotheropoda; 8 Coelophysidae; 10 Averostra; 11 Ceratosauria; 13 Abelisauridae; 14 Tetanurae; 15 Megalosauroidea; 16 Neotetanurae; 17 Allosauroidae; 19 Coelurosauria; 20 Tyrannosauroidea; 23 Tyrannosauridae; 27 Maniraptoriformes; 28 Maniraptora; 31 Clade A; 32; Averemigia; 33 Oviraptoridae; 35 Paraves; 36 Avialae; 37 Deinonychosauria; 38 Dromaeousauridae.

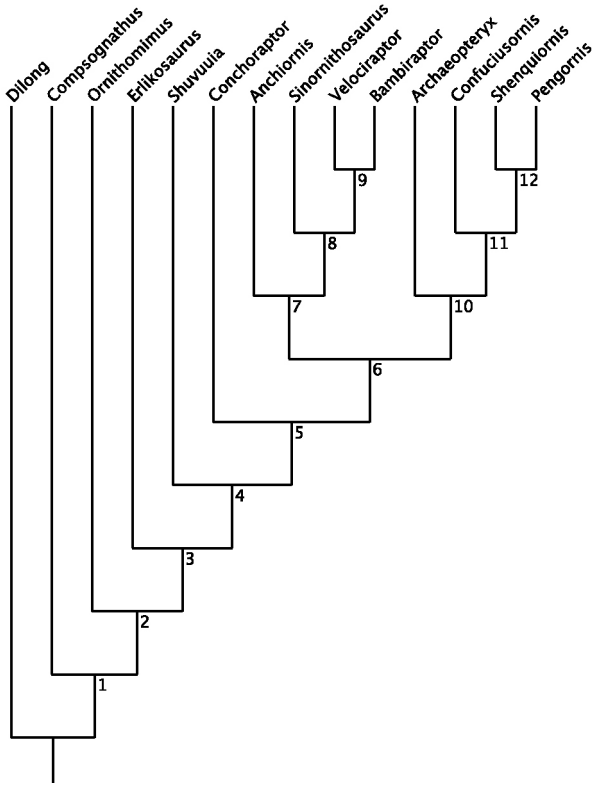

Fig. S4. Topology of the informal supertree used for the small data set. 2 Maniraptoriformes; 3 Maniraptora; 5 Aviremigia; 6 Paraves, 7 Deinonychosauria; 8 Dromaeosauridae; 10 Avialae; 11 Pygostylia; 12 Enantiornithes

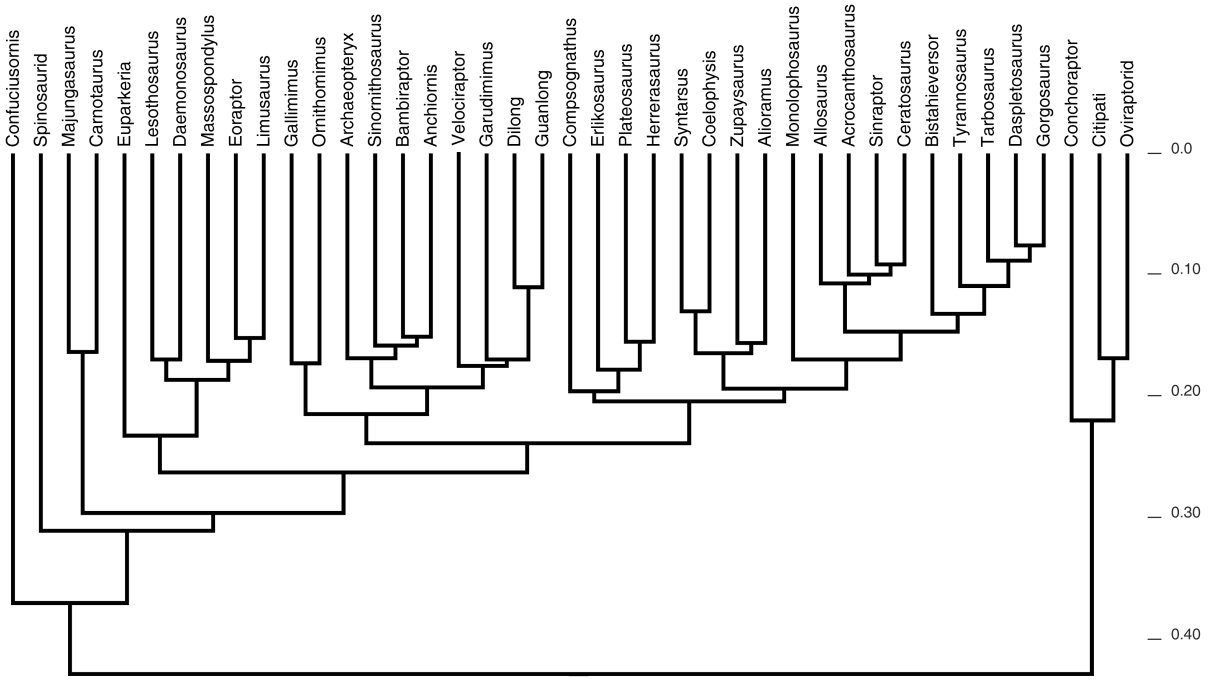

Fig. S5. UPGMA Cluster based on morphometric data. Numbers on the right side represent the distance.

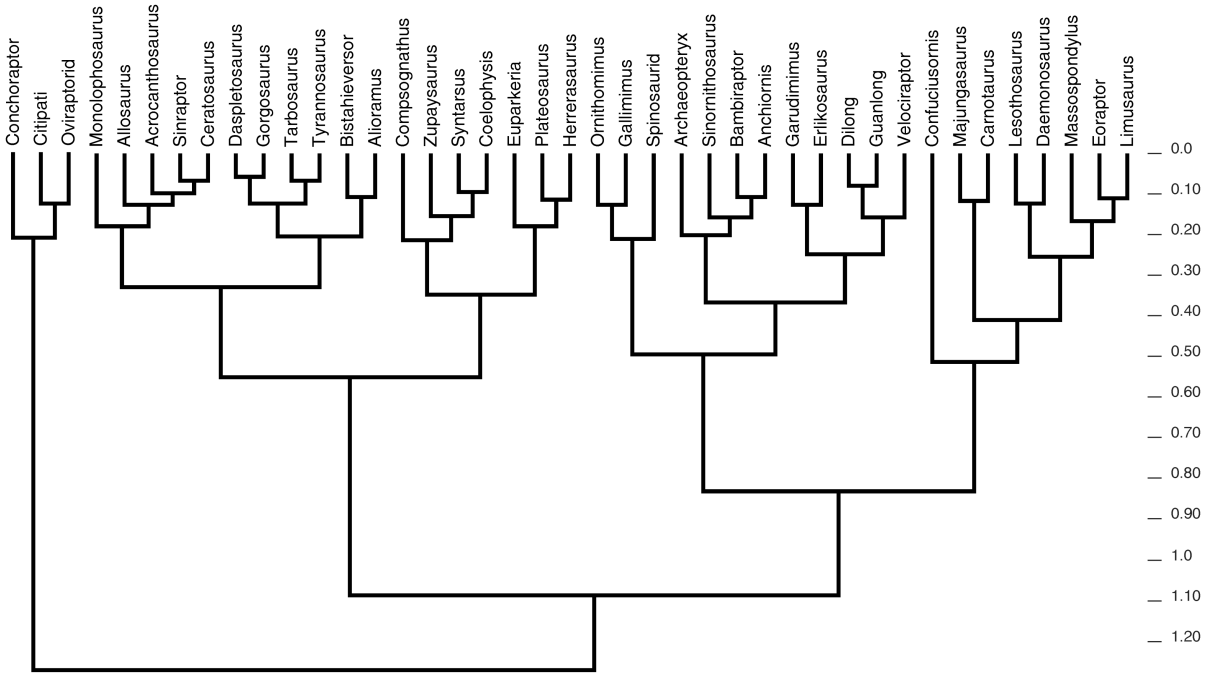

Fig. S6. Ward Cluster based on morphometric data. Numbers on the right side represent the distance.

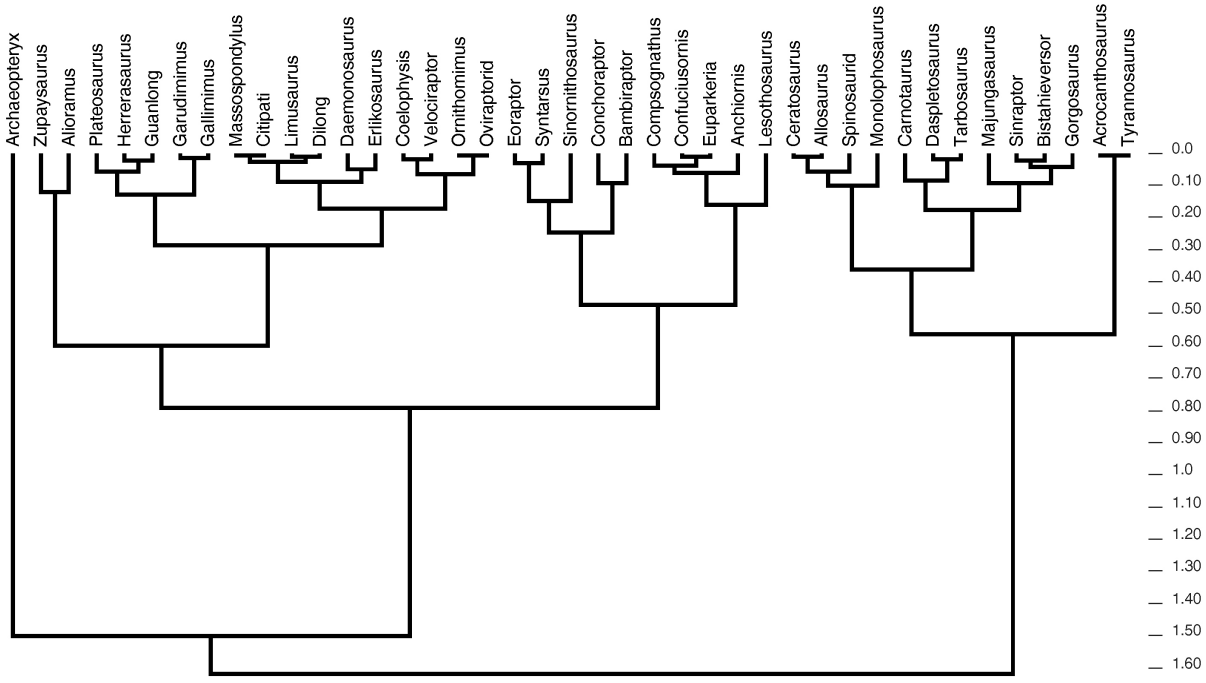

Fig. S7. UPGMA cluster based on skull strength indicator (log transformed). Numbers on the right side represent the distance.

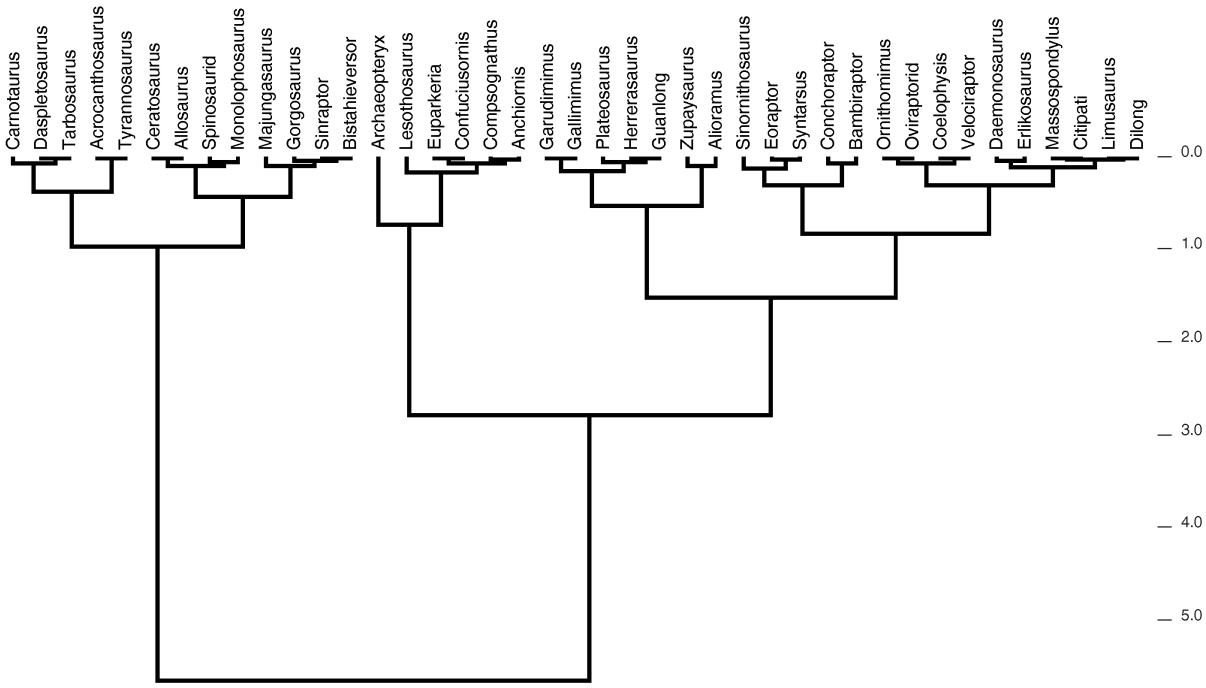

Fig. S8. Ward cluster based on skull strength indicator (log transformed). Numbers on the right side represent the distance.

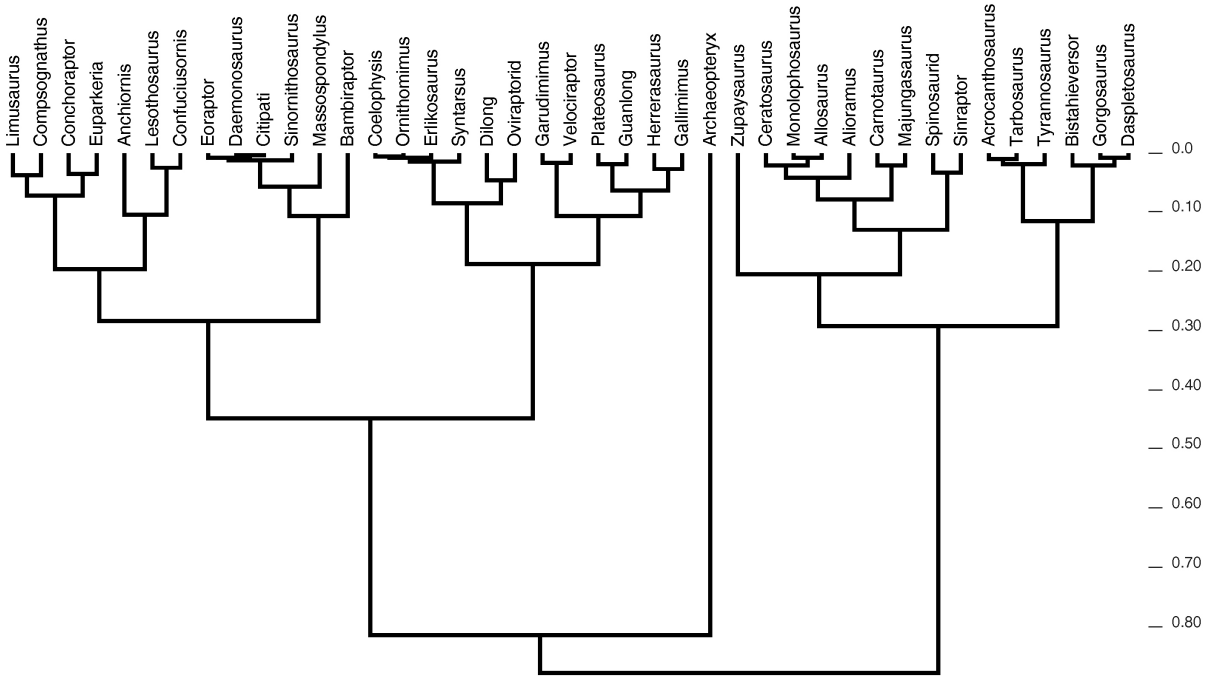

Fig. S9. UPGMA cluster based on average maximum stress (log transformed). Numbers on the right side represent the distance.

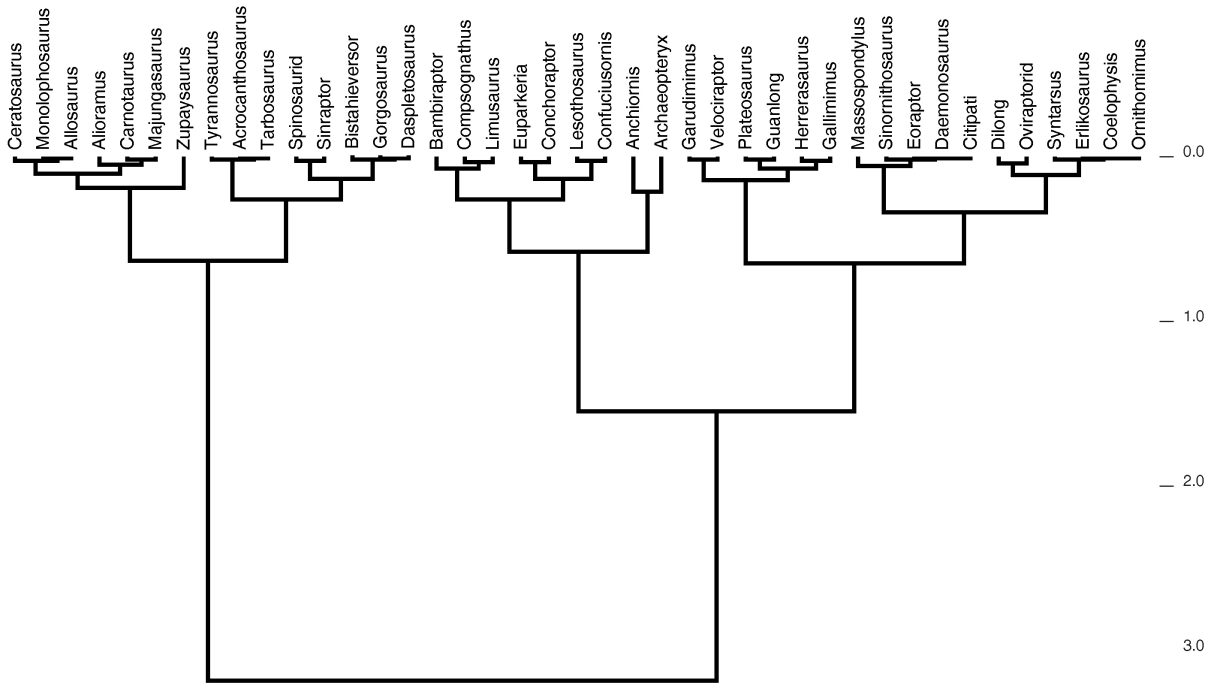

Fig. S10. Ward cluster based on average maximum stress (log transformed). Numbers on the right side represent the distance.

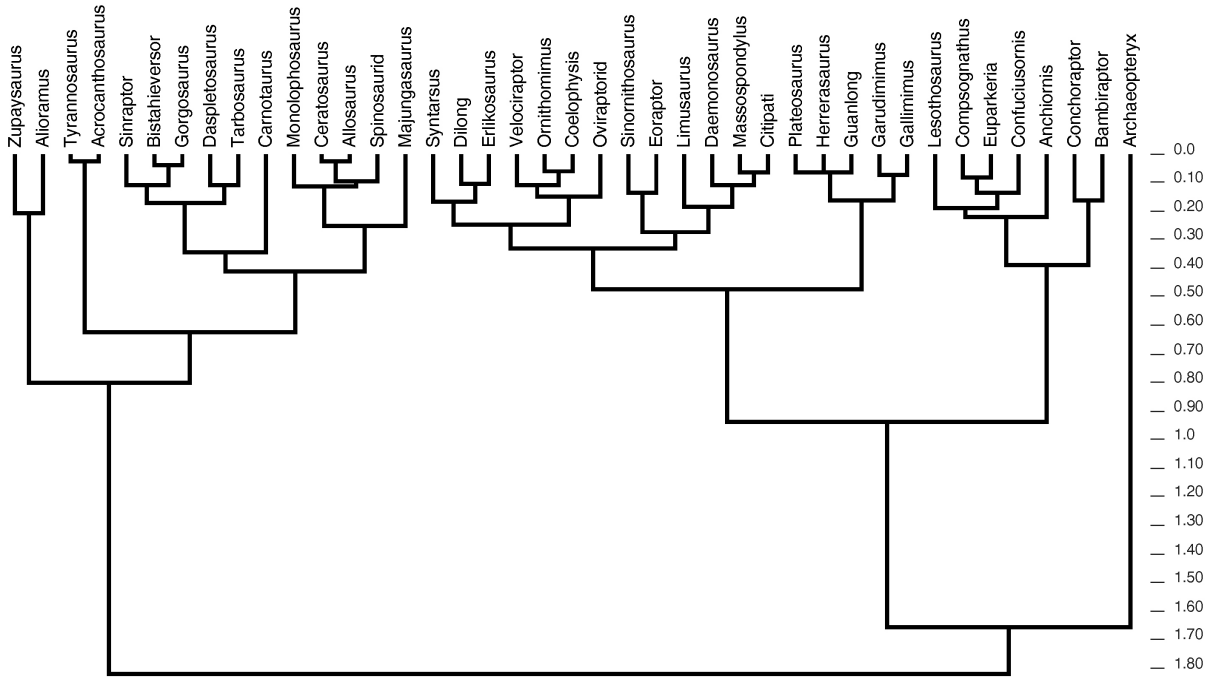

Fig. S11. UPGMA cluster based on skull strength indicator and average maximum stress (both log transformed). Numbers on the right side represent the distance.

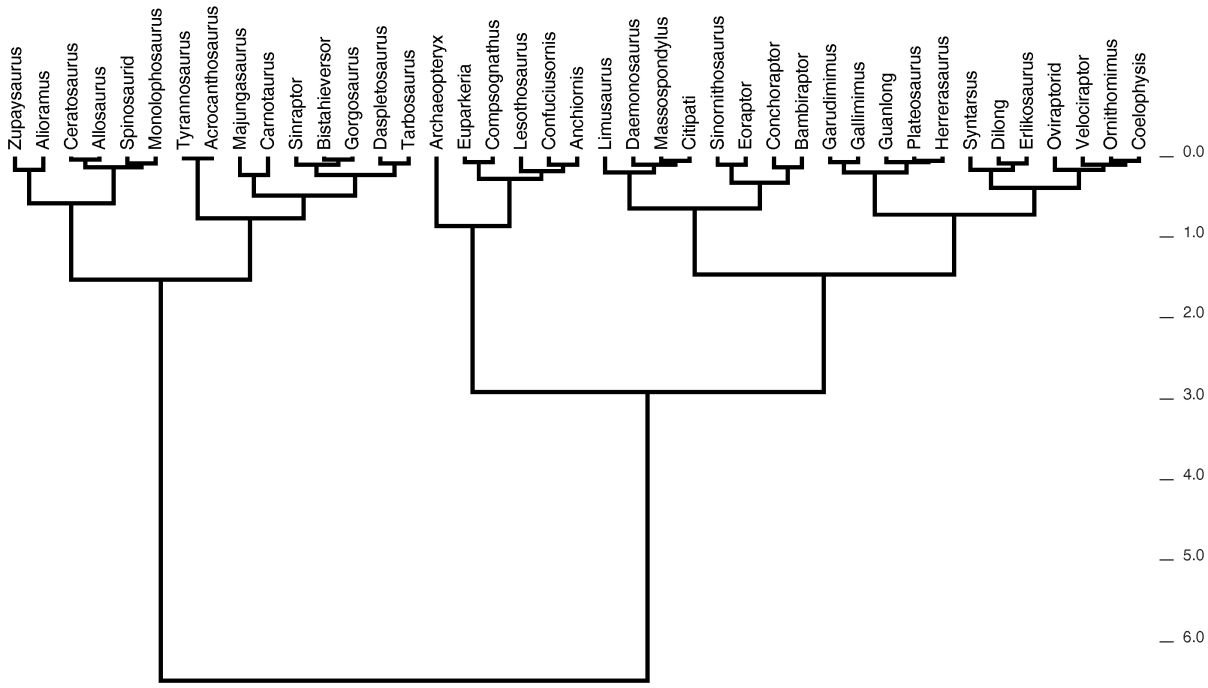

Fig. S12. Ward cluster based on skull strength indicator and average maximum stress (both log transformed). Numbers on the right side represent the distance.

Diet cluster

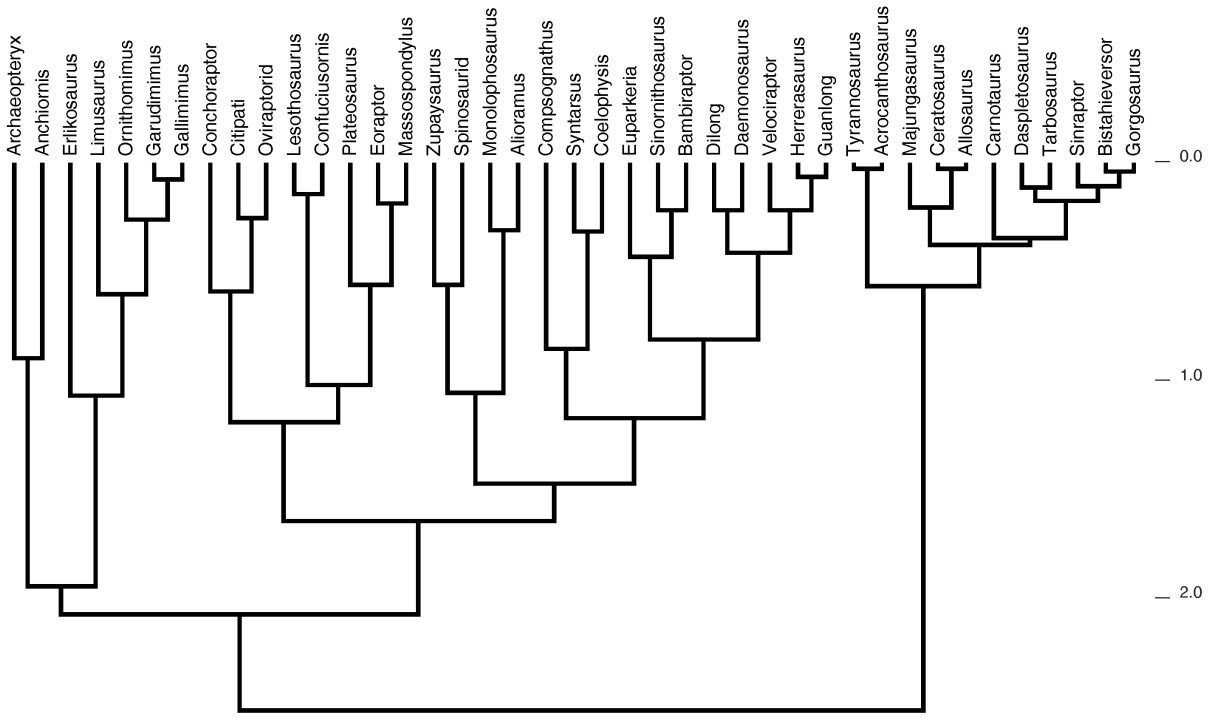

Fig. S13. UPGMA cluster based on feeding ecology, skull strength indicator and average maximum stress (both log transformed). Numbers on the right side represent the distance.

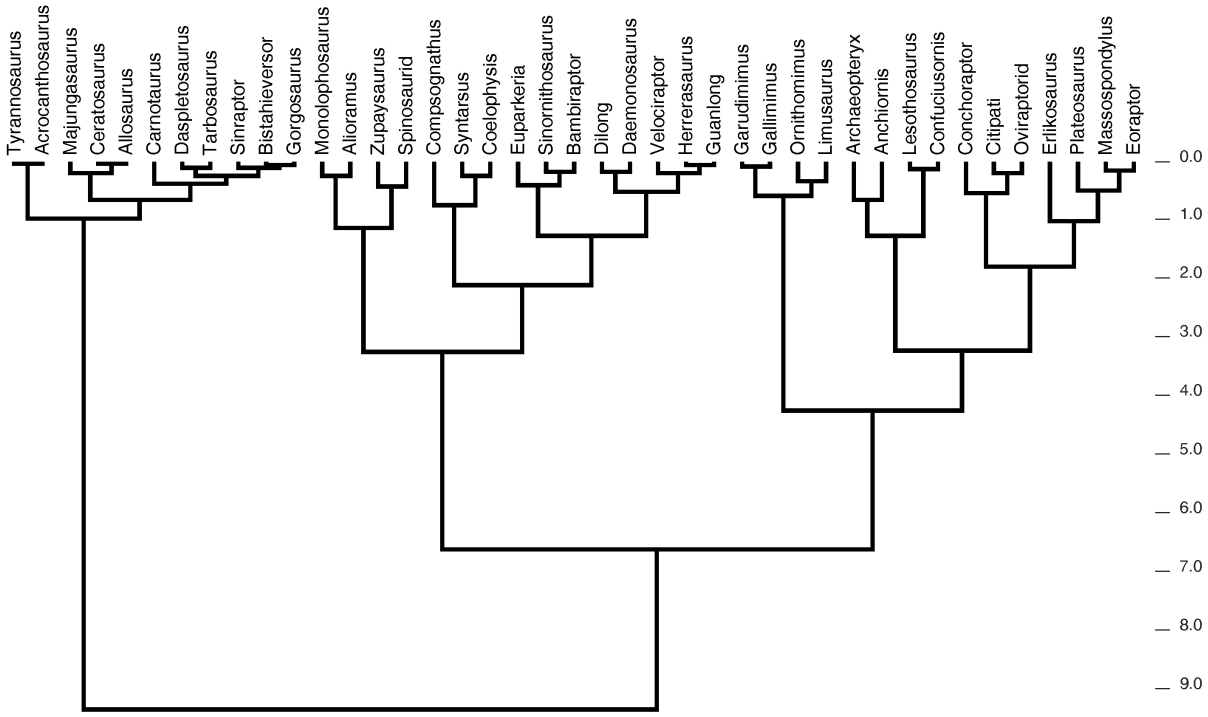

Fig. S14. Ward cluster based on feeding ecology, skull strength indicator and average maximum stress (both log transformed). Numbers on the right side represent the distance.

5. Phylogenetic signals of functional proxies (SSI and AMS) and diagnostic test for PIC analysis

Both morphometric data and functional factors (SSI and AMS) show a phylogenetic signal (Fig. S7). After transforming the scores into PIC values, we first analysed if they fulfil the four criteria listed in the materials and methods section (Table S4). Here, PC 1 and 2 as well as SSI and AMS show no significant correlations. For PC 3 a correlation is present for the fourth criterion (estimated node values vs. the corrected node high). However, as the fourth test indicates primarily evolutionary trends and it is not strictly diagnostic (Midford et al. 2005), all scores can be modelled as random walk with a uniform rate of change, and thus, fulfil the assumptions for PIC analyses. In contrast, the SSI based on Henderson's (2002) original data posses a significant correlation with the first criterion (standard deviation). However, this could be the result of the small sample size.

Table S4. Diagnostic test of the contrasts of PC, logSSI and logAMS scores. Degree of correlation and significance are given by R^2 and *p*-value. * represents the small data set which includes only the original data from Henderson et al. (2002).

	Standard deviation	**PIC node value**	**PIC node high**	**PIC node value vs. PIC node high**
PC 1	0.009/0.554	0.035/0.245	0.002/0.794	0.02/0.388
PC 2	0.009/0.564	0.0003/0.921	0.0022/0.773	0.022/0.357
PC 3	0.032/0.266	0.056/0.14	0.022/0.366	0.563/<0.001
logSSI	0.0004/0.897	0.08/0.077	0.007/0.621	0.026/0.322
logAMS	0.052/0.156	0.175/0.007	0.002/0.788	0.003/0.626
PC 1*	0.048/0.496	<0.001/0.927	0.339/0.047	0.010/0.761
PC 2*	0.377/0.034	0.291/0.070	<0.001/0.995	0.051/0.479
PC 3*	0.100/0.316	<0.001/0.970	<0.001/0.983	0.543/0.006
logSSI*	0.438/0.019	0.251/0.097	0.032/0.580	0.177/0.174

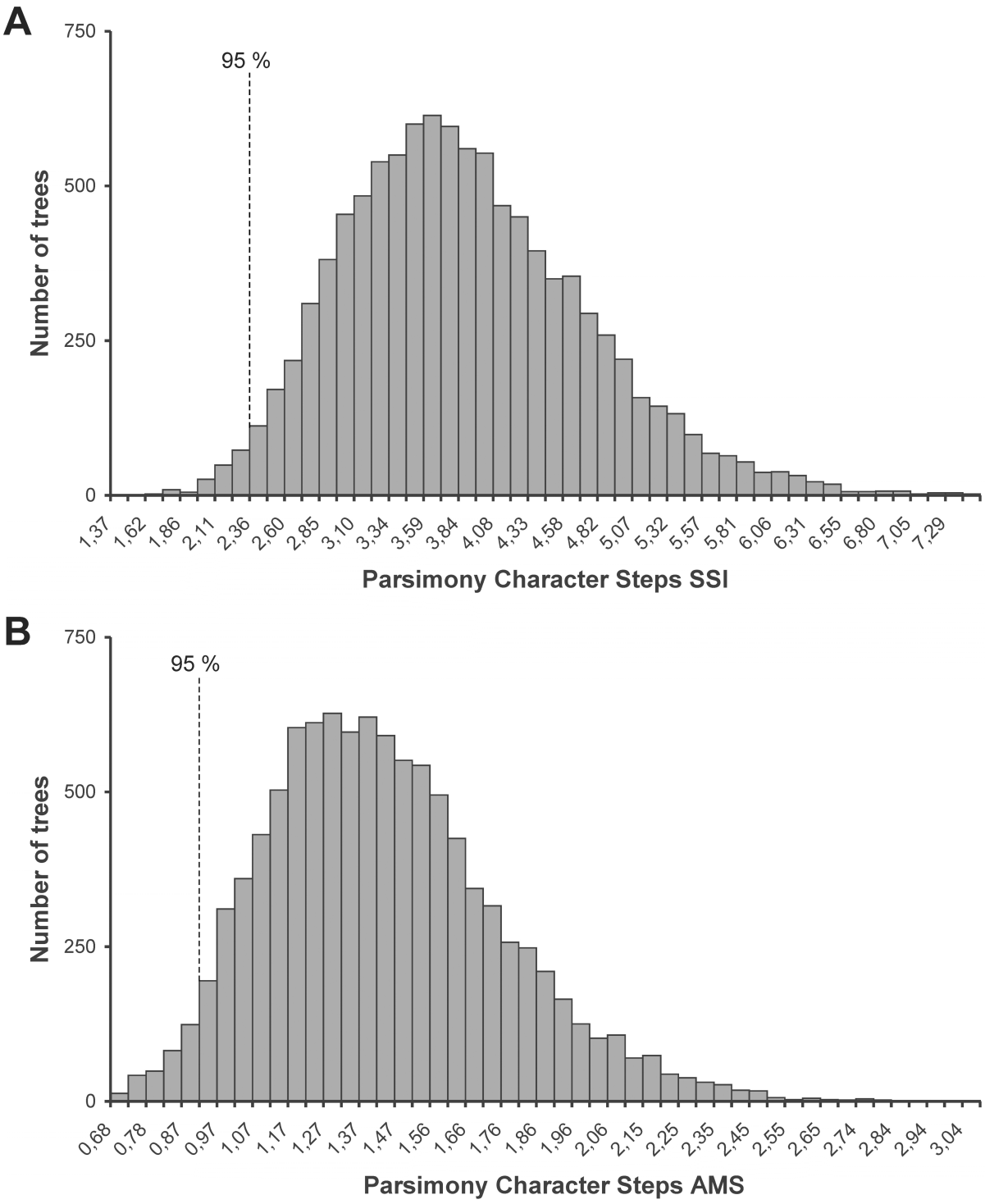

Fig. S15. Results from the permutation test for morphofunctional proxies skull strength indicator (SSI) and average maximum stress (AMS). **A.** Permutation of the skull strength character (logarithmic transformed) showing that the squared length of the supertree (= 0.987) is smaller than in 95 % of the 10 000 simulated tree topologies indicating that the skull strength indicator is phylogenetic constrained. The asterisk marks the 95% border. **B.** Permutation of the average maximum stress character (logarithmic transformed) showing that

the squared length of the supertree (= 0.685) is smaller than in 95 % of the 10 000 simulated tree topologies indicating that the bite force is phylogentic constrained.

6. References

Barsbold, R. and Osmólska, H. 1999. The skull of *Velociraptor* (Theropoda) from the Late Cretaceous of Mongolia. *Acta Palaeontologica Polonica* 44: 189-219.

Brusatte, S.L., Carr, T.D., Erickson, G.M., Bever, G.S., and Norell, M.A. 2009. A long-snouted, multihorned tyrannosaurid from the Late Cretaceous of Mongolia. *PNAS* 106: 17261-17266.

Brusatte, S.L., Benson, R.B.J., Currie, P.J., and Zhao, X. 2010. The skull of *Monolophosaurus jiangi* (Dinosauria: Theropoda) and its implications for early theropod phylogeny and evolution. *Zoological Journal of the Linnean Society* 158: 573-607.

Brusatte, S.L., Sakamoto, M., Montanari, S., and Harcourt Smith, W.E.H. in press. The evolution of cranial form and function in theropod dinosaurs: insights from geometric morphometrics.

Burnham, D.A. 2004. New information on Bambiraptor feinbergi (Theropoda: Dromaeosauridae) from the Late Cretaceous of Montana. *In*: P.J. Currie, E.B. Koppelhus, M.A. Shugar, and J.L. Wright (eds.), *Feathered dragons*, 67-111. Indiana University Press, Bloomington.

Carr, T.D. and Williamson, T.E. 2010. *Bistahieversor sealeyi*, gen. et sp. nov., a new tyrannosauroid from New Mexico and the origin of deep snouts in Tyrannosauroidea. *Journal of Vertebrate Paleontology* 30: 1-16.

Chiappe, L.M., Ji, S., Ji, Q., and Norell, M.A. 1999. Anatomy and systematics of the Confuciusornithidae (Theropoda: Aves) from the Late Mesozoic of northeastern China. *Bulletin of the American Museum of Natural History* 242: 1-89.

Chiappe, L.M., Norell, M.A., and Clark, J.M. 2002. The Cretaceous, short-armed Alvarezsauridae: *Mononykus* and its kin. In: L.M. Chiappe, and L.M. Witmer (eds.), *Mesozoic Birds: Above the heads of dinosaurs*, 87-120. University of California Press, Berkeley.

Colbert, E.H. 1989. The Triassic dinosaur *Coelophysis*. *Museum of Northern Arizona Bulletin* 57: 1-160.

Currie, P.J. and Zhao, X. 1993. A new carnosaur (Dinosauria, Theropoda) from the Jurassic of Xinjiang, People's Republic of China. *Canadian Journal of Earth Sciences* 30: 2037-2081.

Eddy, D.R. and Clarke, J.A. 2011. New information on the cranial anatomy of *Acrocanthosaurus atokensis* and its implications for the phylogeny of Allosauroidea (Dinosauria: Theropoda). *PLoS ONE* 6: e17932.

Erickson, G.M., Lappin, A.K., and Vliet, K.A. 2003. The ontogeny of bite-force performance in American alligator (*Alligator mississippiensis*). *Journal of Zoology, London* 260: 317-327.

Ezcurra, M.D. 2007. The cranial anatomy of the coelophysoid theropod *Zupaysaurus rougieri* from the Upper Triassic of Argentina. *Historical Biology* 19: 185-202.

Galton, P.M. 1985. Cranial anatomy of the prosauropod dinosaur *Plateosaurus* from the Knollenmergel (Middle Keuper, Upper Triassic) of Germany. *Geologica et Palaeontologica* 19: 119-159.

Gow, C.E., KItching, J.W., and Raath, M.A. 1990. Skulls of the prosauropod dinosaur *Massospondylus carinatus* Owen in the collections of the Bernand Price Institute for Palaeontological Research. *Palaeontologia Africana* 27: 45-58.

Henderson, D.M. 2002. The eyes have it: The sizes, shapes, and orientations of theropod orbits as indicators of skull strength and bite force. *Journal of Vertebrate Paleontology* 22 (4): 766-778.

Holtz, T.R. Jr. 2004. Tyrannosauroidea. *In*: D.B. Weishampel, P. Dodson, and H. Osmólska (eds.), *The Dinosauria*, 111-136. University of California Press, Berkeley.

Hu, D., Hou, L., Zhang, L., and Xu, X. 2009. A pre-*Archaeopteryx* troodontid theropod from China with long feathers on the metatarsus. *Nature* 461: 640-643.

Hurum, J.H. and Sabath, K. 2003. Giant theropod dinosaurs from Asia and North America: skulls of *Tarbosaurus bataar* and *Tyrannosaurus rex* compared. *Acta Palaeontologica Polonica* 48: 161-190.

Langer, M.C. 2004. Basal Saurischia. *In*: D.B. Weishampel, P. Dodson, and H. Osmólska (eds.), *The Dinosauria*, 25-46. University of California Press, Berkeley.

Makovicky, P.J., Kobayashi, Y., and Currie, P.J. 2004. Ornithomimosauria. *In*: D.B. Weishampel, P. Dodson, and H. Osmólska (eds.), *The Dinosauria*, 137-150. University of California Press, Berkeley.

Norman, D.B., Witmer, L.M., and Weishampel, D.B. 2004. Basal Ornithischia. *In*: D.B. Weishampel, P. Dodson, and H. Osmólska (eds.), *The Dinosauria*, 325-334. University of California Press, Berkeley.

O'Connor, J.K. and Chiappe, L.M. 2011. A revision of enantiornithine (Aves: Ornithothoraces) skull morphology. *Journal of Systematic Palaeontology* 9 (1): 135-157.

Osmólska, H., Currie, P.J., and Barsbold, R. 2004. Oviraptorosauria. *In*: D.B. Weishampel, P. Dodson, and H. Osmólaka (eds.), *The Dinosauria*, 165-183. University of California Press, Berkeley.

Peyer, K. 2006. A reconsideration of *Compsognathus* from the Upper Tithonian of Canjuers, southeastern France. *Journal of Vertebrate Paleontology* 26 (4): 879-896.

Rauhut, O.W.M. 2003. The interrelationships and evolution of basal theropod dinosaurs. *Special Papers in Palaeontology* 69: 1-213.

Rayfield, E.J. 2011. Structural performance of tetanuran theropod skulls, with emphasis on the Megalosauridae, Spinosauridae and Charcharodontosauridae. *Special Papers in Palaeontology* 86: 241-253.

Rohlf, F.J. 2005. TpsDig2. Department of Ecology and Evolution, State University of New York, Stony Brook, New York.

Sampson, S.D. and Witmer, L.M. 2007. Craniofacial anatomy of *Majungasaurus crenatissimus* (Theropoda: Abelisauridae) from the Late Cretaceous of Madagascar. *Journal of Vertebrate Paleontology* 27: 32-102.

Sues, H.-D., Nesbitt, S.J., Berman, D., and Henrici, A.C. 2011. A late-surviving basal theropod dinosaur from the latest Triassic of North America. *Proceedings of the Royal Society B* 278: 3459-3464.

Tykoski, R.S. 1998. *The osteology of Syntarsus kayentakatae and its implications for ceratosaurid phylogeny*. 217 pp., The University of Texas, Austin.

Xu, X. and Wu, X. 2001. Cranial morphology of *Sinornithosaurus millenii* Xu et al. 1999 (Dinosauria: Theropoda: Dromaeosauridae) from the Yixian Formation of Liaoning, China. *Canadian Journal of Earth Sciences* 38: 1739-1752.

Xu, X., Norell, M.A., Kuang, X., Wang, X., Zhao, Q., and Jia, C. 2004. Basal tyrannosauroids from China and evidence for protofeathers in tyrannosauroids. *Nature* 431: 680-684.

Xu, X., Clark, J.M., Forster, C.A., Norell, M.A., Erickson, G.M., Eberth, D.A., Jia, C., and Zhao, Q. 2006. A basal tyrannosauroid dinosaur from the Late Jurassic of China. *Nature* 439: 715-718.

Xu, X., Clark, J.M., Mo, J., Choiniere, J., Forster, C.A., Erickson, G.M., Hone, D.W.E., Sullivan, C., Eberth, D.A., Nesbitt, S., Zhao, Q., Hernandez, R., Jia, C., Han, F., and Guo, Y. 2009. A Jurassic ceratosaur from China helps clarify avian digital homologies. *Nature* 459: 940-944.